June 1985 LRP 263/85

STUDY OF THE IDEAL MHD STABILITY LIMIT FOR JET

H. Saurenmann, S. Semenzato, S. Succi,
R. Gruber and F. Troyon

FINAL REPORT

Contract JB1/9018

STUDY OF THE IDEAL MHD STABILITY LIMIT FOR JET

I) INTRODUCTION

The α particle heating power in JET fueled with 50%-50% DT, at the full field of 3.5 T and a full aperture plasma, can be approximated[1] by

$$P_\alpha \approx \beta^2, \tag{1}$$

where β is the volume averaged β in % and the power P_α is in megawatts. The objective is to obtain significant α particle heating. An α-power of 5 to 10 MW for an auxiliary heating power of 25 MW would appear to be already a very significant result. It would require a β between 2.2 and 3.2%, corresponding to an energy confinement time $\tau_E = 11\ \beta/(25 + \beta^2)$ (β in %) between 0.7 and 1 second always with 25 MW of heating. Although these values of β seem at first sight modest since they have been experimentally exceeded in Doublet III[2] and they lie far below the limits predicted from ideal MHD stability considerations[3,4], it is not clear that they can be reached with the JET parameters. In both the experimental and theoretical studies made so far, record values of β coincide with record low q values, while JET is a low current, high q device. Since the required confinement time would be within reach if there were no degradation from the ohmic value, the existence of a β limit and how much it is, has become an important issue. Evenmore, as the dilution effects due to impurities further enhance the β required to reach the same α-power production.

The goal of this study is to provide input to this problem of a limiting β, focusing on some well-defined objectives, namely to find, within the frame of ideal MHD,

a) the highest β that can be reached with the parameters specified for full performance

b) the sensitivity of the β limit to a change of the current

c) the effect of the vacuum vessel on the β limit for the full performance range of parameters.

The only differences between this study and those already published are: the choice of the class of profiles and the additional constraint that the maximum β is found at constant current.

To fully specify an equilibrium, two arbitrary functions of the magnetic flux ϕ must be given. They can be the pressure $p(\phi)$ and the current flux $T(\phi) \equiv rB_\phi$ (r is the radius, B_ϕ the toroidal field), or the pressure p and the safety factor $q(\phi)$. Specifying the q profile is very convenient for the ballooning mode analysis and pressure optimisation, and it is commonly used without much elaboration on the difficulty that it leads generally to a non-vanishing current density at the edge with high probability of free boundary instabilities. Specifying the derivatives, p' and TT', is more traditional and allows one to enforce simply the constraint of vanishing current at the edge. In all but one[2] of the previous studies, p' and TT' have been chosen proportional to each other, which implied that the pressure profile was more peaked than the current profile[3,4,5]. It was the simplest assumption and there was no reason to do otherwise as it was thought to be good for stability[6].

In the present study we also specify the profiles of p' and TT' but we retain more general parametric forms for the two functions in order to be able to vary independently the profiles to obtain the highest stable β. With hindsight from this study, but also from other studies we have carried out since the achievement of this work, it has become clear that it is best to have a narrow current profile and a wide pressure profile. This explains the difference between the older results and these new results.

The plan of the paper is as follows: Section II describes the configuration and the class of profiles over which the optimisation is carried out. The results are in Section III while Section IV contains a discussion of the results and of their reliability.

II) PARAMETRISATION OF THE EQUILIBRIA

The plasma surface is assumed to be profile and current independent, and given by the parametric expressions

$$r = r_p(\theta) \equiv R + a\cos(\theta + \delta\sin\theta)$$

$$z = z_p(\theta) \equiv Ea\sin\theta, \tag{2}$$

where $-\pi \leq \theta \leq \pi$ is the running parameter, r and z the horizontal and vertical coordinates, and R, a, E and δ the major radius, the horizontal half-width, the elongation and the triangularity respectively. A good approximation to the boundary shown in the «JET project description EUR5516e», known also as R-5, is obtained for

$$R = 2.96m,\ a = 1.25m,\ \delta = 0.3,\ E = 1.68. \tag{3}$$

We shall use these values throughout.

There is no evidence that the detailed plasma shape is important for stability but this should be considered as still an open question on which we shall come back in the discussion.

The vessel plays the role of a conducting shell with a time constant much larger than the typical ideal MHD time scale of a microsecond. Because of its structure consisting of alternating high and low resistivity sections, it is not truly axisymmetric. On the fast time scale, it can nevertheless be considered as an axisymmetric perfectly conducting shell. For convenience, the shell is represented by the equations

$$r = r_p(\theta) + (\Delta r_1\cos^2\frac{2\theta}{2} + \Delta r_2\sin^2\frac{2\theta}{2})\cos\theta$$

$$z = z_p(\theta) + \Delta z\sin\theta \tag{4}$$

where θ is same parameter as in eq. (2).

where the parameters Δr_1 and Δr_2 are the distances between the plasma and the inside and outside wall in the mid-plane respectively and Δz the plasma-wall distance at the maximum elongation. We have used as standard values $\Delta z = \Delta r_1 = 16$ cm and $\Delta r_2 = 20$cm.

The most crucial choice is that of the profiles. The Grad-Shafranov equation for the flux $\psi(r,z)$ is written

$$\frac{\partial^2\psi}{\partial z^2} + \psi \frac{\partial}{\partial r}\left(\frac{1}{r}\frac{\partial\psi}{\partial r}\right) = -rj = -r^2 \frac{dp}{d\psi} - T\frac{dT}{d\psi}, \qquad (5)$$

where j is the toroidal current density and $T \equiv rB_\phi$. We choose the normalisation such that $\psi \equiv 0$ is on the surface. The two source functions are represented by polynominals

$$\frac{dp}{d\psi} = \sum_{n=1}^{N_p} p_n \psi^n$$

$$T\frac{dT}{d\psi} = \sum_{n=1}^{N_t} t_n \psi^n \qquad (6)$$

On the plasma boundary, p' and TT' vanish, so that $j \equiv 0$, which is believed to be a necessary condition for stability[7]. But it is not certain that one should have identically $j = 0$ on the boundary rather than just the flux surface average $\langle j \rangle = 0$, since the argument is based on the lowest order term in the standard Tokamak expansion of the energy principle in which only flux average quantities appear. This is still an open question to be studied.

The number of terms in the expansions must be limited for obvious reasons. Most of the studies reported here have been done with $N_t = 1$ and $N_p = 2$. This is the same choice as in the INTOR studies[8] which allows useful comparisons. Attempts at introducing more terms have been generally unsuccessful in terms of β limit. They will be described in Section IV. With the 3 free parameters t_1, p_1 and p_2 we can play on the pressure profile while keeping the total current

I constant and the volume average $\beta \equiv \int p dv / \int B^2/2 dv$ constant. A limit to this choice of parameters becomes obvious at very low β, when the pressure gradient no longer contributes significantly to the current density so that there remains in fact only one parameter t_1 and it is fixed by the total current. There is no longer any free parameter to optimise stability, for example by changing the safety factor on axis q_o. We shall only be confronted with this difficulty at high current and it is then necessary to increase the number of terms in TT' to adjust the value of q_o which appears to be a key parameter for stability.

Since the stability character of an equilibrium does not depend on density, we shall always assume it to be a constant ρ_o. For convenience, the equilibrium solver uses normalized quantities which we label with an index E:

$$R_E = 1, \quad a_E = a/R = 0.423, \quad I_E \equiv \mu_o I/B_\phi R, \tag{7}$$

where B_ϕ is the vacuum toroidal field at radius R.

III) THE METHOD AND ITS LIMITATIONS

Low-n stability is studied with ERATO[9], a spectral code which solves the variational form of the linearized ideal MHD equations. The eigenvalue Γ^2 is related to the growthrate γ by the relation

$$\Gamma^2 = \gamma^2 R_m^2 / V_{Am}^2 \tag{8}$$

where R_m is the radius of the magnetic axis and V_{Am} the Alfvén velocity at the same radius.

The displacement eigenvector $\underline{\xi}$ is represented as

$$\underline{\xi} = (\xi_n^1 \cos n\Phi + \xi_n^2 \sin n\Phi)\hat{\underline{n}} + (\underline{\xi}_t^1 \cos n\Phi + \underline{\xi}_t^2 \sin n\Phi), \tag{9}$$

where $\hat{\underline{n}} = \underline{\nabla}\psi/|\underline{\nabla}\psi|$, Φ is the toroidal angle, $\underline{\xi}_t$ is the component of $\underline{\xi}$ tangential to the magnetic surface and the integer n the toroidal index.

The origin of Φ is chosen such that the vector $(\xi_n^1, \underline{\xi}_t^2)$ is up-down antisymmetric and $(\xi_n^2, \underline{\xi}_t^1)$ up-down symmetric. This is possible because only up-down symmetric equilibria are considered here.

We only search for the most unstable mode. Since, in all cases of interest, there is at least one singular surface within the plasma, the spectrum of eigenfrequencies ω^2 (ω is the frequency of the mode) has a stable continuum part which extends to the marginal point, namely $\omega^2 = 0$. Stability can thus only be marginal. But the discretisation scheme used in ERATO leads, at least for all Tokamak profiles studied so far, to a destabilisation of the spectrum, so that a convergence study of the growthrate of the most unstable mode as a function of mesh size must in principle be done and, if the equilibrium is stable, it should converge to the marginal point. Since the marginal point is a pathological degenerate singular mode, which causes an irregular convergence, and the numerical accuracy is limited by the numerical resolution and the power of the computer, we make use of the concept of σ-stability introduced by J.P. Goedbloed and P.H. Sakanaka[10] with some additional constraints. For n = 1 an equilibrium is declared stable if, simultaneously, $|\Gamma^2| < 10^{-4}$ with a fixed resolution of 60 x 60 meshcells over the full cross-section, Γ^2 drops rapidly with increasing resolution and the mode pattern has the structure expected of a continuum mode with dominant shear motion on singular surfaces. This last criterion has been used in the past as the sole criterion to identify a continuum destabilized mode but any weakly growing mode has a structure which resembles a continuum mode.

The σ-stability threshold has been chosen for the following reasons. Below $\Gamma^2 = 10^{-4}$ convergence becomes generally irregular, due either to the fact that the mode belongs to the continuum and the plasma is thus stable or to the insufficient definition of the equilibrium or maybe even to the approach of the limit of accuracy of the computer which shows when calculating some second derivatives of equilibrium quantities required as input by ERATO. In cases where a great

effort has been made to increase the resolution, the growthrate has decreased further at least as long as $q_o > 1$. At such small growthrates, with such highly sheared flow patterns, the validity of the physical model as well as the assumptions of axisymmetry, no flow and pressure isotropy, should be questioned. The internal kink at $q_o < 1$ is the only documented example where we know[11] that the growthrate can be below this σ-threshold. This means the σ-stability limit below $q_o < 1$ should be considered optimistic.

For $n > 1$, resolution should be increased accordingly. For $n = 2$, to have the same reliability, we should then use 120 x 120 mesh, which is an impossibility with present computers. It means that results with $n > 1$ should be considered with some caution.

We make use of two different versions of ERATO. They differ in the way the vacuum potential energy is calculated. The first one[9] uses a Green function formulation and it can handle exactly the case of an infinite vacuum region. This is the version used in most of the $n = 1$ calculations and, when not specified, it should be understood that this version has indeed been used. There is another version in which the vacuum region around the plasma is dealt in the same way as the plasma itself[12]. This necessitates that a shell be placed around the plasma to limit the domain. There are definite advantages to this version as soon as n increases and it is better suited to the case where there is a shell than the Green function version. We shall mention explicitely when this version is used, designating it as the discretized vacuum ERATO (DVERATO). In this version, there is an option to use a ballooning mode presentation which permits to keep the same azimuthal discretisation for all n, but the radial resolution must still increase linearly with n to resolve all singular surfaces and the resolution of the equilibrium then becomes the limiting factor. But we only have limited experience yet with this option when there is a vacuum region so that we have not been able to use its full potential in this problem.

Stability to ballooning modes ($n = \infty$) is studied with a one-dimensional energy principle on a large number of magnetic surfaces (usually 60 to 100)[9]. The domain of integration on each surface is

extended to $\pm\infty$, corresponding to turning an infinite of times around the surface, in the standard fashion. Practically, the number of turns is limited by the accuracy of the equilibrium and of the computer. In most cases, because of the elongation, D shape and small aspect ratio, unstable modes exhibit strong ballooning on the outside so that a few turns are sufficient to localize the ballooning unstable region. But in the vicinity of the magnetic axis or in the regions of low shear, when the q profile is flat or has a minimum, the largest number of turns which can be used (100) is not sufficient, as evidenced by the fact that the Mercier unstable range of magnetic surfaces is sometimes found ballooning stable, which is known to be impossible. To alleviate this difficulty, we verify the Mercier criterion on the same set of magnetic surfaces and assume that, if after so many turns, the ballooning criterion is not violated, the destabilizing contribution to the potential energy must come mainly from the asymptotic region, the sign of the contribution of which is tested by the Mercier criterion, and thus that the Mercier and ballooning criterion should give almost the same result. This difficulty is common knowledge[13] and more acute in configurations with negative shear $dq/d\psi < 0$, such as in spheromaks where the same prescription is used[14].

IV) RESULTS

a) JET Full Performance

The parameters which characterize full performance are B_ϕ = 3.5 T and I = 4.8 MA. The corresponding normalized values in the equilibrium code are

$$B_{\phi E} = 1 \text{ and } I_E = \mu_o I/T = 0.5822. \qquad (10)$$

A large number of equilibria have been generated which cover densely a large area in the $(p_2/p_1,\ t_1/p_1)$ plane. The resolution was generally 140/70 radial/vertical mesh cells with a few cases at 200/100. Only the upper-half cross-section is calculated. In this study, $N_p = 2$ and $N_t = 1$ so that there is one equilibrium for each point in the plane $(p_2/p_1,\ t_1/p_1)$.

The standard version of ERATO has been run, without a shell, for n = 1, using a 60/60 mesh (full cross-section) with radial and azimuthal redistribution of the mesh points to resolve the singular surfaces and have enough points in the outer region of the plasma near the plasma surface where the non-orthogonal mesh opens up (see for example figure 2). Figure 1 shows in the plane (p_2/p_1, t_1/p_1) the lines of constant normalized growthrate Γ, starting from $\Gamma^2 = 10^{-4}$ which is the σ-stability limit. Also shown are lines of constant q on axis, q_o, and constant β. These lines are obtained by interpolation between the values calculated. The highest σ-stable β is slightly above 3% and is reached for $q_o \sim 1.1 - 1.15$. The shapes of the constant Γ lines are all similar, with the optimum less pronounced as Γ increases, but always located in the range $q_o \sim 1.1 - 1.15$. There is an obvious difference in behaviour below and above $q_o \sim 1$. Below, the stability limit looks more like a limitation on the current density on axis such as would be expected from an internal kink instability, while above $q_o \sim 1$, it is a β limit with some q_o dependence. Figure 2 shows a sequence of unstable modes with increasing growthrate, starting with one very close to the σ-marginally stable mode. The 3 equilibria have almost the same q_o but different β. As β increases, the mode becomes more global and faster growing, while the peaking of the tangential component of flow at the singular surfaces becomes less visible. Because of the high shear at the edge associated with the D-shape (at the surface $q_s \sim 6.5 - 7.5$), there is a large number of singular surfaces packed together. Surprisingly, the growthrate has been found rather insensitive to the radial resolution in the outer region, at least for q_o near the optimum. It means the high shear at the edge has no stabilizing influence in this case, implying the mode balloons across the high shear edge and it must be the core of the plasma which drives the instability.

There remains to verify the other two criteria on the $\Gamma^2 = 10^{-4}$ line to use this as a σ-stability threshold: the mode must look like a singular mode and Γ^2 must decrease rapidly as the number of mesh points increase. The sequence of modes in figure 2 shows how a singular mode is approached although it is not as singular as found in the INTOR study[8] for the same Γ^2 of 10^{-4}. Increasing the resolution decreases Γ^2 and further peaks the mode on singular surfaces.

The ballooning stability limit B is shown in Fig. 3, together with the Mercier limit (M) on the axis, the most dangerous point for that criterion, and the σ-stability limit of the n=1 external mode redrawn in the plane (q_o,β) instead of the original plane $(p_2/p_1, t_1/p_1)$.

When B is crossed by increasing β, the first magnetic surface to become unstable is somewhere between the axis and the surface. As β increases, the unstable range of magnetic surfaces widens. The exact limit is obtained already with a few turns indicating a strong ballooning of the modes. As q_o increases above 2.3, the maximum value shown in Fig. 3, the ballooning limit still increases and at $q_o = 3.75$, the largest value for which we have been able to generate an equilibrium, the limit is at $\beta = 5\%$. Figure 4 shows a sequence of equilibria lying along the stability boundary B on the unstable side to show the location of the dangerous regions.

When q_o drops below M an unstable range develops around the axis. It is a second ballooning unstable range which we cannot find directly with the ballooning code. The modes must be localized interchanges. It explains why the M and B limits cross instead of having B smoothly joining M on the low β side. The two limits are in fact two ballooning limits in different regions, one with strongly, the other with weakly ballooning modes.

Figure 5 shows a sequence of n = 1 σ-marginal equilibria with different q_o. It shows that shear is good for the stability of this mode, provided q_o remains above 1. The optimal case C_2 has a $\beta \sim 3\%$ while on axis $\beta_o \sim 10.6\%$.

The dependence on q_o of the M, B limits and of the n = 1 free boundary limit are quite different at $q_o > 1$, but they recover each other at $q_o < 1$, giving the feeling that this region is inaccessible even though the limit appears soft. This is a point to be discussed later.

The ballooning limit can be as well above or below the n = 1 free boundary limit. We have not identified any specific feature of the

profile related to the n = 1 free boundary limit so that we cannot manipulate this limit to bring it above the ballooning limit at high q_o. But near the optimum on the free boundary limit at $q_o \sim 1.1\text{-}1.15$, we can imagine local changes in the pressure profiles, shifting some of the pressure gradient away from the dangerous region, which push the ballooning limits up and to the left so that the n = 1 free boundary optimum at 3.1% becomes ballooning stable.

The stability of the n > 1 modes is difficult to determine, as explained earlier. We have nevertheless tried to determine the trend and understand the transition from the n = 1 to the n = ∞ stability limit. In these studies, we use the version DVERATO, placing the conducting shell at a distance $\Delta z = \Delta r_1 = 3.75$ m and $\Delta r_2 = 1.30$ m, large enough that it does not affect the n = 1 limit, thus a fortiori the higher ns. It is not possible to use the σ-stability criterion for the same resolution 60 x 60 as for n = 1. We do a coarse convergence, taking up to 80 x 80 mesh and packing points radially near the surface, in the high shear region, to resolve the singular surfaces, and we declare stability when the extrapolation to zero mesh size is below 10^{-4}. At this time, we cannot do better and one cannot overemphasize too much how careful one should be in using these results, particularly the n = 4. But the great similarity between these results and those obtained in the INTOR study[8], where the situation is better because of the larger aspect ratio and lower shear, gives some confidence that the main results are general. They are shown in Fig. 6. The essential result is that the low n > 1 modes do not give a lower limit on β than the kink and ballooning together.

For comparison, the rigid boundary modes n = 1, 2 and 4 are also shown. It seems that all modes become unstable in a narrow range of q_o and β which does not leave much hope of an improvement by a more clever choice of profiles.

In conclusion the highest value of β at which there is full stability is at the intersection of the n = 1 and n = ∞ limits and is $\beta_{max} = 2.8\%$. By a small adjustment of the profile of the pressure it should be possible to bring the ballooning limit above the highest

point of the n = 1 limit, and β_{max} would then be slightly over 3%. Note that the scaling law we have proposed[16] with the INTOR value of the coefficient

$$\beta_{max} = 2.2 \frac{\mu_o I}{a B_\phi} \qquad (11)$$

would give 3%.

b) Variation of the current

We have repeated the calculation for the n = 1 free boundary limit and for the n = ∞ ballooning limit with different values of the current. The parameter range has been restricted to the vicinity of the optimum, around q_o = 1. The results are shown in Fig. 7. The threshold of σ-stability of the kink is the same for all cases. The largest current is 9.6 MA. The general behaviour is the same in all cases and the same as found in our INTOR study[8]. For 12 MA the n = 1 limit still behaves as expected with a maximum at β = 7.2% but the ballooning criterion becomes violated over the full range of β studied, down to β = 5.5%. This case will be discussed later in section 4 and is not shown in Fig. 7.

We did not repeat the calculation of the n > 1 modes, because of the time involved and of the uncertainty attached to such a calculation which cannot be made with sufficient resolution.

Figure 8 summarizes the results. For each current, two values of the limiting β are shown: the maximum β stable to n = 1 free-boundary and Mercier, and the maximum β stable to all n. At low current, there is no doubt that the pressure profile can be modified slightly to bring the ballooning limit at the level of the n = 1 optimum, but at the highest current it is by no means certain and we shall discuss it for the highest current we have tried, 12 MA, in the next section.

The line drawn through the points in Figure 8 is the Lausanne scaling law[16] with the INTOR coefficient quoted above (eq. 11). There is a difficulty at high current already mentioned in the introduction. With the choice of $N_t = 1$, q_o falls below one above a current of about 4.8 MA at $\beta = 0$. As the current is increased above this value, a new instability region appears at low β. The stable domain then becomes a band with a high and a low β limit. It is the additional freedom brought by the p' terms, which can be used to bring q_o above 1, that creates the lower stability boundary. This instability region at low β can be suppressed completely by introducing an additional term in TT' which keeps q from dropping below one everywhere, taking for example $N_t = 2$. But as the current keeps increasing, N_t should increase further to avoid local minima of q below one somewhere in the plasma. This is cumbersome and one has to recognize that the polynominal expressions (6) are inadequate at high current. This difficulty is purely numerical as previous calculations[4] have shown that equilibria at $\beta = 0$ can be stable down to $q_s = 2$. This is the reason why the lower boundary is not shown in figures 7 and 8 and that the highest current considered is 12 MA, corresponding to $q_s \approx 2.4$.

c) Wall stabilisation

The vacuum vessel fits the plasma so tightly that the n = 1 free-boundary mode is fully stabilized. It is not unreasonable to expect that the ballooning limit M+B is the limit in this case, although we cannot run the higher ns to verify that they are all stabilized by the wall. To make effective use of the stabilizing influence of the wall to increase β, it is necessary to be able to maintain as flat a q profile as possible. As long as $q_o \approx 1$, there is no gain with the profiles considered here. Our polynominal expressions are not suited to an optimisation of the pressure profile to the ballooning criterion alone because of the local character of such an optimisation and the global character of the polynominals. We have not pursued further this study.

V) DISCUSSION

a) Increase of parameter space

We have not made systematic tries to increase N_p and N_t in the source terms (6). But we did spend a substantial effort to study the case of 12 MA and since the general behaviour is qualitatively the same at low current we shall describe our attempts in this case.

The starting point was an equilibrium with a $\beta = 7.25\%$ slightly above the maximum of the $n = 1$ σ-stability line. The equilibrium quantities p, q, $dp/d\psi$, $T(dT/d\psi)$ and j are shown in Fig. 9. It is ballooning unstable. The normalized growthrate squared, Γ^2, of the $n = 1$ kink is 2×10^{-4} with the standard 60/60 mesh and is not far from the σ-stability limit. The q profile is hollow with $q_o = 1.32$ and $q_{min} = 1.16$.

The first objective was to introduce one more term in each of the source terms [6] to try to stabilize this equilibrium while keeping β = constant. Let us introduce a term t_2, keeping t_1/p_1, p_2/p_1 and I constants. We find that Γ^2 ($n = 1$) has a parabolic dependence with the minimum very close to $t_2 = 0$ so that there is nothing to gain.

Introducing a term p_3 has the same effect as t_2 but the growthrate increases much faster as $|p_3|$ increases away from the optimum at $p_3 \approx 0$ than with t_2, for the same change of q_o. This evolution is in agreement with the evolution described in section 3: for the stability of the $n = 1$ free-boundary mode it is best to have q_o just above 1 to maximize the average shear; it is best to avoid peaking of the pressure on axis as much as possible. The case considered is in this respect very close to the optimum which explains our inability to improve on the $n = 1$ limit.

Since the optimum equilibrium for $n = 1$ is ballooning unstable let us first repeat the full optimisation with $N_p = 2$ and $N_t = 1$ in order to find a fully stable equilibrium. Figure 10 shows the σ-stability limit for the $n = 1$ kink in the same plane as Fig. 1, namely t_2/p_1 and p_2/p_1. The lines of constant β are also visible

near the limit. Shown also on the graph are two lines corresponding to the onset of ballooning modes in two different regions of the plasma. To the left of B2 there is one unstable region as shown in Fig. 9. As B2 is crossed, the Mercier criterion becomes violated on axis because of increasing q_o. When p_2/p_1 increases, the outside unstable region located around the maximum of the pressure gradient $|p'|$ shrinks and disappears as B1 is crossed. But at the same time q_o keeps increasing, with the q profile becoming more and more as in a screw-pinch, so that the Mercier and ballooning criteria are violated over the central region of the plasma. This is the reason there is no point corresponding to full stability in Fig. 8 for this value of the current. This is illustrated in Fig. 11 in which the same equilibrium quantities as in Fig. 9 are shown for these equilibria, identified in Fig. 10 as E2 to E4. The equilibrium E1 is the one shown in Fig. 9.

Looking at the Mercier and ballooning unstable regions, it is immediate that the central unstable region can be suppressed by enforcing $p' = 0$ in the central region. To keep the current profile and total current unchanged, the loss in current which results from setting $p' = 0$ in the center must be compensated by adding the same amount to $-TT'$. The loss in β will be very small since the change in pressure on axis is given by $\delta p_{axis} = 2\int \delta p' s ds$, which is small since p' appears multiplied by s, and integration of this small change over the small central volume will give a minute change in β. This means that the limit B1 should be considered the ballooning limit. The $n = 1$ limit should be unaffected by this reduction which does not change the current profile.

Above B1 one might also try to reduce the intermediate unstable range by some small modifications of the profiles. In the equilibria E1, E2 and E3, the unstable region is located around the maximum of $|p'|$. By shaving off the top of the $-p'$ curve and again replacing the current lost by an equivalent contribution to TT', all these equilibria should become ballooning stable. It is noteworthy to remark that the threshold for the ballooning instability in this region is about the same for the 3 equilibria, $|p'| \approx 1$ to 1.15. In the equilibrium E2 the shaving of the top should lead to an insignificant drop in the β

of 6.50%. For E1 the shaving at $|p'| = 1.15$ would lead to a more important reduction, but since β for that equilibrium is 7.5%, it should still be around 7%. None of these modifcations are expected to destabilize the kink n = 1 so that full stability should be possible at around 7%, the optimum for n = 1. The key is to keep the current density unaffected as much as possible while making small changes to the pressure profile.

To shift the pressure gradient outwards from the ballooning unstable region instead of reducing it, to keep β constant, is a possibility which has not been tried. It would be necessary in this case to check the stability of the n = 1 mode. Shifting the pressure gradient inwards is less effective in terms of keeping β constant.

It is clear from this description that the polynomial expansion is totally inadequate for these adjustments which must be local. We have made numerous attempts to add terms in (6) to stabilize the ballooning modes and find the β limit for full stability without success. For the n = 1 mode we do not have a localized criterion so that we do not know if localized changes could also be done to improve the β limits.

b) Influence of the shape

The shape has been kept fixed through these calculations. Yet we know that the representation used is only an approximate convenient form. How sensitive are the results on the shape, specially on details?

ERATO does not allow in its present form locally non-convex shapes. Also the coordinate system becomes skewed when the shear is very high. This makes it impossible to study fully this problem. There is nevertheless some evidence in our calculations which suggest that details may not be important. With the present shape already, shear is very large at the edge of the plasma at low current as visible in Figs. 4 and 5. Many singular surfaces lie close together on the outer edge already at the nominal 4.8 MA. In principle, the mesh should be

sufficiently dense to resolve all these surfaces in order to trust the results. But for the n = 1 runs, we have not seen significant differences as far as the stability limit is concerned between a rough and a good resolution of these singular surfaces. It is this remark which gave us the courage to run higher ns for which we cannot resolve suffiently well all the singular surfaces. We take this as circumstantial evidence that details of the shape which strongly influence the shear at the edge are not important.

Another evidence is naturally the agreement between the scaling law (11) and the experimental results, some of which have been obtained with odd shapes as in DIII.

VI. CONCLUSIONS

Ideal MHD stability limits the β that can be achieved. The stability of free-boundary modes impose a limit on β as well as that of internal ballooning modes. Optimisation of the ballooning mode stability alone leads to flat q profiles, unlike those that are observed. Optimisation of the n = 1 free-boundary mode stability leads to a q profile with q_o near one, namely with the maximum shear compatible with the internal kink stability requirement. This optimum corresponds to the naturally occurring q profile. For this optimum profile all modes (all n) seem to become unstable at about the same value of β. The results are, within 10%, in agreement with the scaling law (11) proposed in[16] up to the highest current studied of 12 MA.

No claim is made that another optimisation with different source functions could not lead to higher β with the same type of q profiles. But it should also be noted that in a stationary purely ohmic regime there is a constraint between the pressure and current profile, which could result in a lower β limit than that found here.

It might be interesting to examine the implications of these results on the α heating power one could expect.

The expression (1) for P_α has been obtained by making a number

of assumptions: the plasma is a pure 1:1 DT mixture, the velocity distributions are Maxwellian with $T_i = T_e$, the plasma is fully elongated with a volume of 135 m^3 and the average β^2, usually denoted β^{*2}, is 2.6 β^2. We can compare this last assumption with the values found after optimisation in the course of this work.

At 4.8 MA, in the range of parameters near the region of maximum β at 3%, corresponding in Fig. 1 to the region around C2, $(\beta^*/\beta)^2 \sim 2.15$. This is 17% below the assumed 2.6 and it leads to a corresponding reduction in the maximum α power expected.

The corresponding values for the cases of I = 7.2 MA and 9.6 MA are $(\beta^*/\beta)^2 \approx 1.85$ and 1.65. The decrease of B^*/β as the current increases is expected and independent of the optimisation procedure. It reduces the gain in P_α brought by the increase in current, but only slightly.

Acknowledgments

This work has been performed as an Article 14 Contract for JET. Throughout the execution of this contract we have enjoyed constant interaction with the JET theory, in particular with Drs. T. Stringer and J. Wesson.

References

1. A. Gibson, JET-Scientific Council 1/5.
2. Burrett et al., Nucl. Fusion 23 (1983) 536.
3. L.C. Bernard et al., Nucl. Fusion 20 (1980) 1199.
4. W. Kerner et al., Nucl. Fusion 21 (1981) 1283.
5. A.M.M. Todd et al., Nucl. Fusion 19 (1979) 743.
6. INTOR, Phase IIA, European Contr. EUR FU BRU/XII-132/82/EDV30 (1982) 72.
7. J. Wesson, Proc. 7th European Conf. on Turbulated Fusion and Plasma Physis, Vol. 2 (1975) 102.
8. F. Troyon et al., NET Report, EUR XII-324/14, Bruxelles
9. R. Gruber et al., Comp. Phys. Comm. 21 (1981) 323.
10. J.P. Goedbloed and P.H. Sakanaka, Phys. Fluids 17 (1974) 908.
11. W. Kerner et al., Phys. Rev. Letters 44 (1980) 536.
12. R. Gruber et al., Comp. Phys. Comm. 24 (1981) 363.
13. J. Greene and M. Chance, Nucl. Fusion
14. P. Gauthier et al., Nucl. Fusion 11 (1983) 1399.
15. F. Troyon and R. Gruber, LRP 239/84.
16. F. Troyon et al., Plasma Phys. and Contr. Fusion 26 1A (1984) 209.

Figure Captions

Fig. 1: The n = 1 free-boundary iso-growthrate (Γ = const) curves in the p_2/p_1, t_1/p_1 plane. The labels on the curves 10^{-4}, 10^{-3}, 5×10^{-3}, 10^{-2} indicate the corresponding value of Γ^2. The resolution is 60 x 60 (full cross-section).

Fig. 2: Maps of the unstable poloidal flow pattern in two perpendicular meridian planes, $\Phi = 0$ and $\Phi = \pi/2$, for 3 equilibria having the same current and $q_o = 1.15$, with βs of 3.2, 3.5 and 4.1%, identified in figure 1 as A_1, A_2 and A_3.

Fig. 3: The ballooning (B) and Mercier (M) limits in the (q_o,β) plane. Stability is below B and to the right of M. The σ-limit of the n = 1 free boundary mode ($\Gamma^2 = 10^{-4}$) shown in the figure 1 is redrawn in the same plane for comparison.

Fig. 4: Profiles of equilibrium quantities (pressure p, safety factor q, toroidal current density j) in the equatorial plane. The radius R is normalized so that it is 1 on axis. The pressure is normalized to the magnetic pressure on axis $B^2/2$ so that it is very near to the local β. The scale for j is arbitrary. These equilibria are just ballooning unstable to show the location of the first surfaces which become unstable. They are identified in Figure 3 as D1 to D3. The last one, D4, has $q_o = 3.75$ which is outside the scale of Fig. 3. The unstable ranges are shown with the label B.

Fig. 5: Profiles of equilibrium quantities for a set of nearly marginal equilibria, shown in Fig. 1 as C1 to C5. The meaning of the symbols is the same as in Fig. 4.

Fig. 6: The n = 1, n = 2 and n = 4 free-boundary σ-stability limits for I = 4.8 MA, together with the n = 1, n = 2 and n = 4 rigid boundary limits. The rigid boundary cases are labeled with an asterisk.

Figure Captions (cont'd)

Fig. 7: Stability diagrams for increasing values of the current: I = 3.6, 4.8, 6.0, 7.2 and 9.6 MA. The curve labeled 10^{-4} is the free boundary σ-stability limit.

Fig. 8: Dependence of the β limit on current. The line is given by $\beta = 2.2(\mu_o I/aB)$.

Fig. 9: A 12 MA, β = 7.25% equilibrium (E1)

a) Profiles of the source terms p' and TT' and of the pressure p and safety factor q as function of $s = \sqrt{(\psi_{axis}-\psi)/\psi_{axis}}$ (ψ = 0 at the surface) showing the ballooning unstable region.

b) Profiles of p, q and j (arbitrary units) across the equatorial plane. The radius R is normalized to one on the magnetic axis.

Fig. 10: The n = 1 free boundary σ-stability limit and Mercier ballooning limits in the p_2/p_1 and t_1/p_1 plane for a constant current of 12 MA. The resolution is 60 x 60 mesh intervals in the full cross-section.

Fig. 11: Profiles of equilibrium quantities of three 12 MA equilibria, identified as E2, E3 and E4 in Fig. 10, showing the ballooning unstable regions. The corresponding β values are 6.5%, 5.8% and 5.7% respectively.

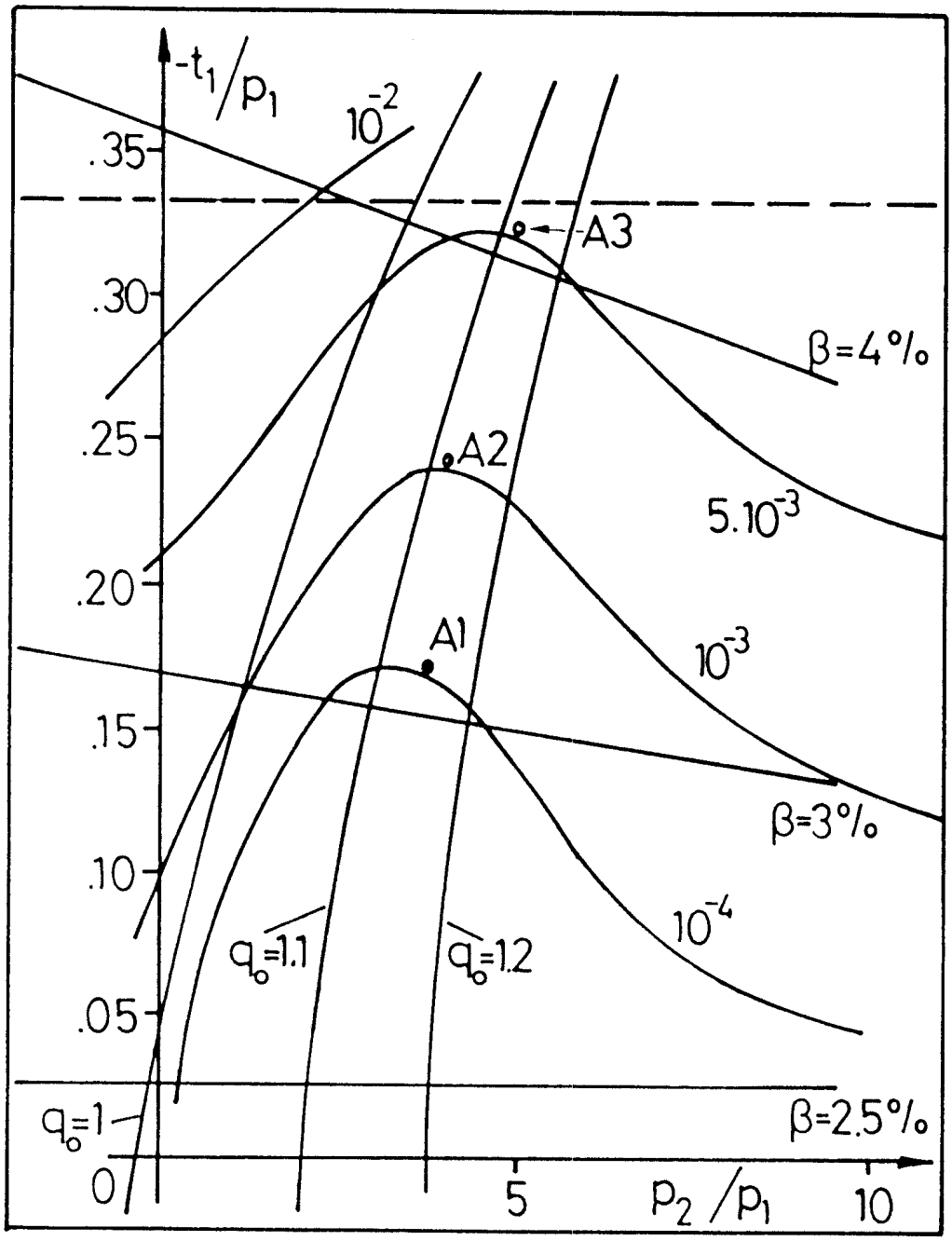
$-t_1/p_1$
10^{-2}
.35
.30
.25
.20
.15
.10
.05
A3
A2
A1
$\beta=4\%$
5.10^{-3}
10^{-3}
$\beta=3\%$
10^{-4}
$q_o=1.1$
$q_o=1.2$
$q_o=1$
$\beta=2.5\%$
0
5
p_2/p_1
10

FIG. 1

JET EQUILIBIRUM A1

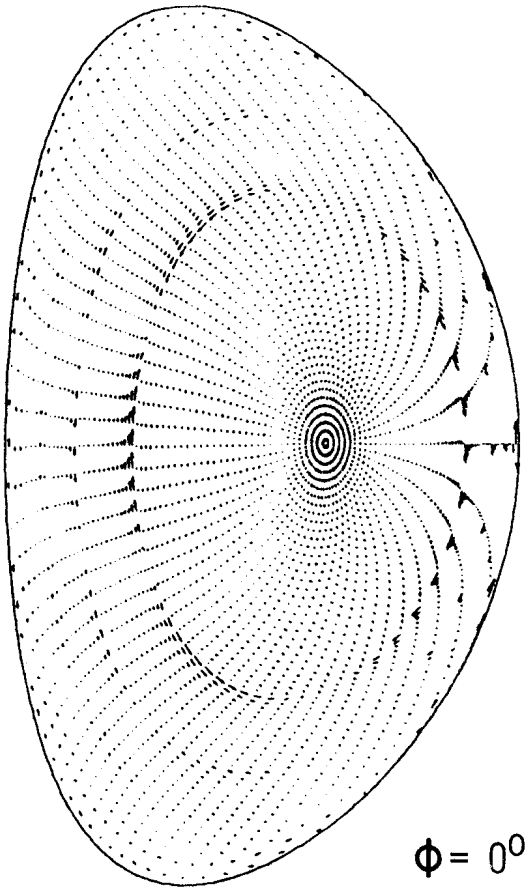

$\phi = 0^{o}$

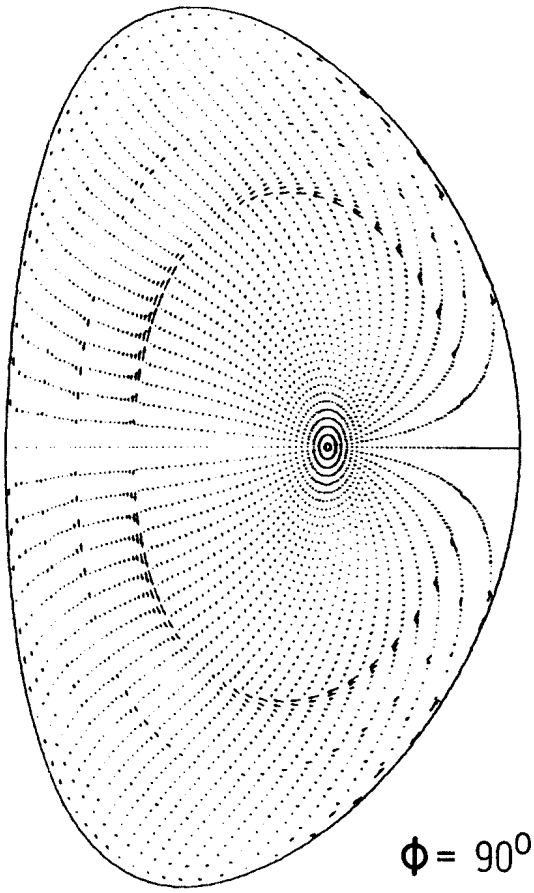

$\phi = 90^{o}$

JET EQUILIBRIUM A2

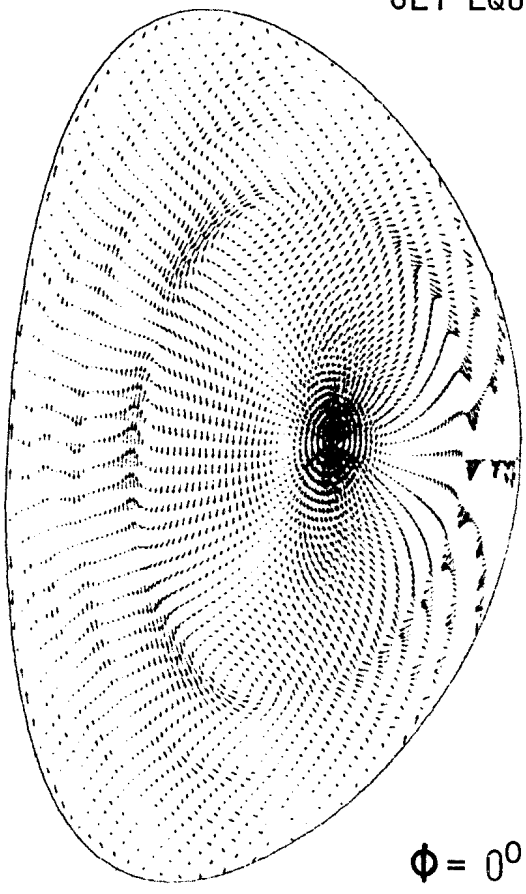

$\phi = 0^{o}$

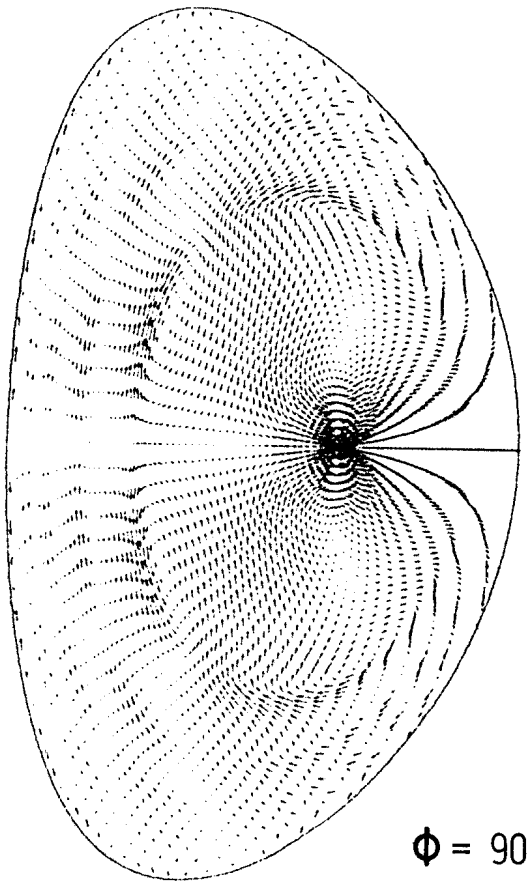

$\phi = 90^{o}$

FIG. 2

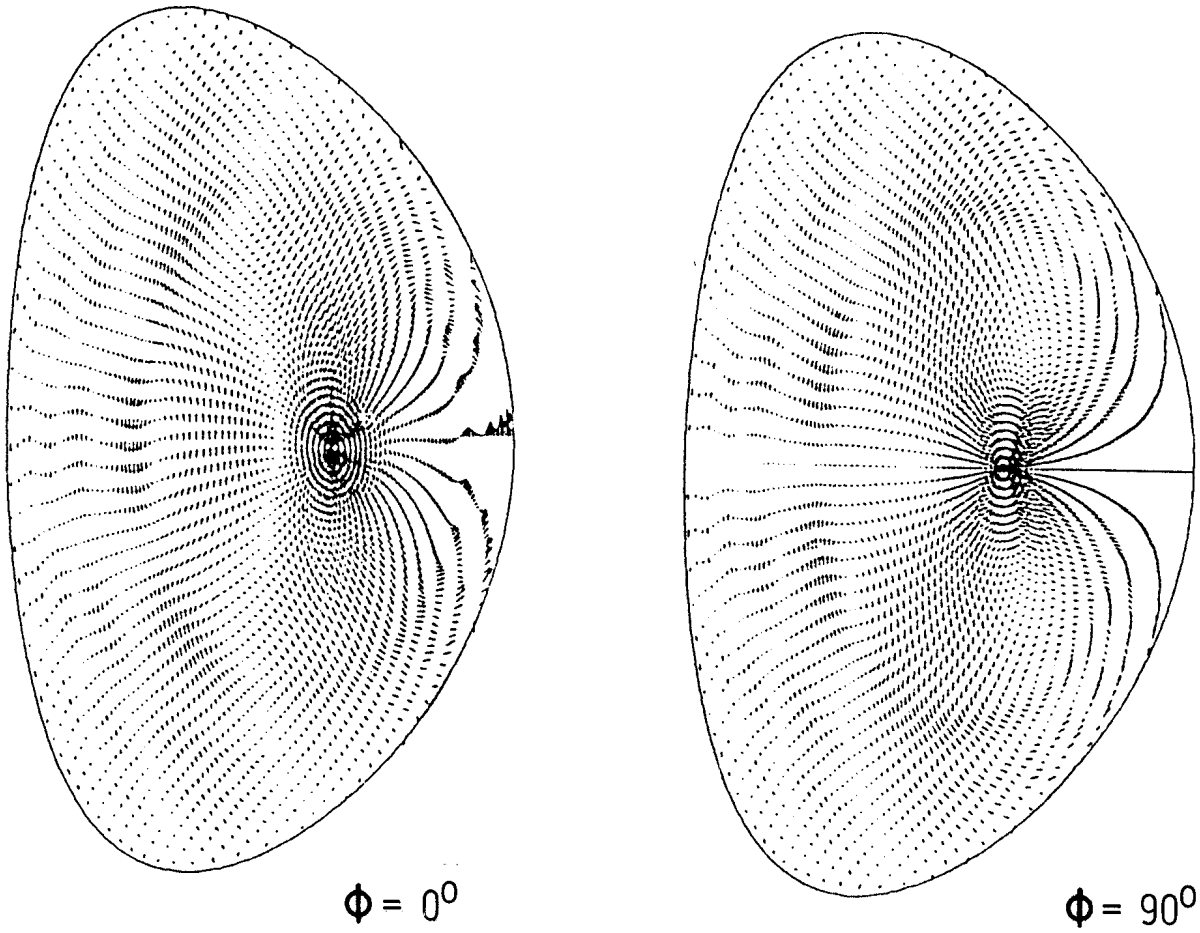

FIG. 2 (CONT'D)

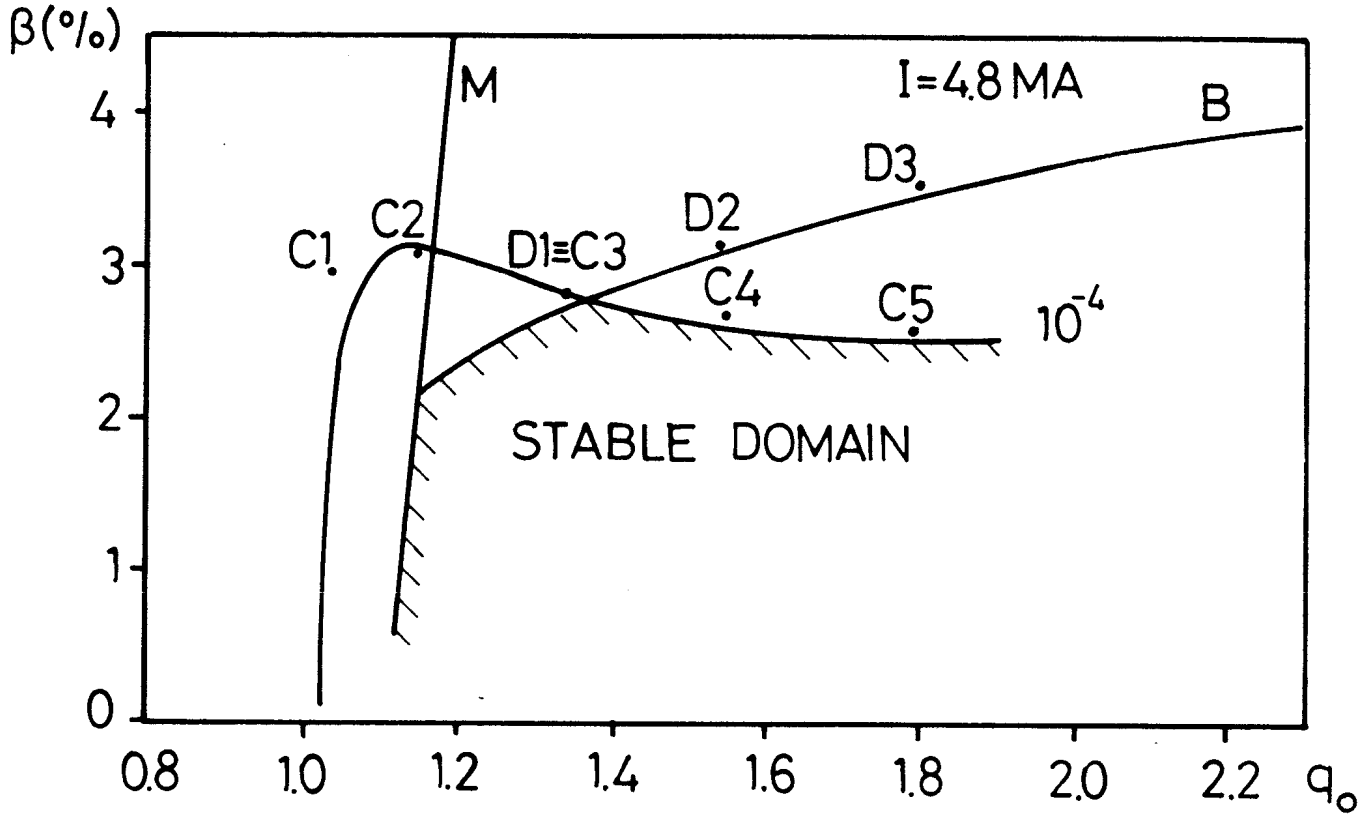
β(%)
4
3
2
1
0
M
I=4.8 MA
B
D3
D2
C1
C2
D1≡C3
C4
C5
10⁻⁴
STABLE DOMAIN
0.8
1.0
1.2
1.4
1.6
1.8
2.0
2.2
q₀

FIG. 3

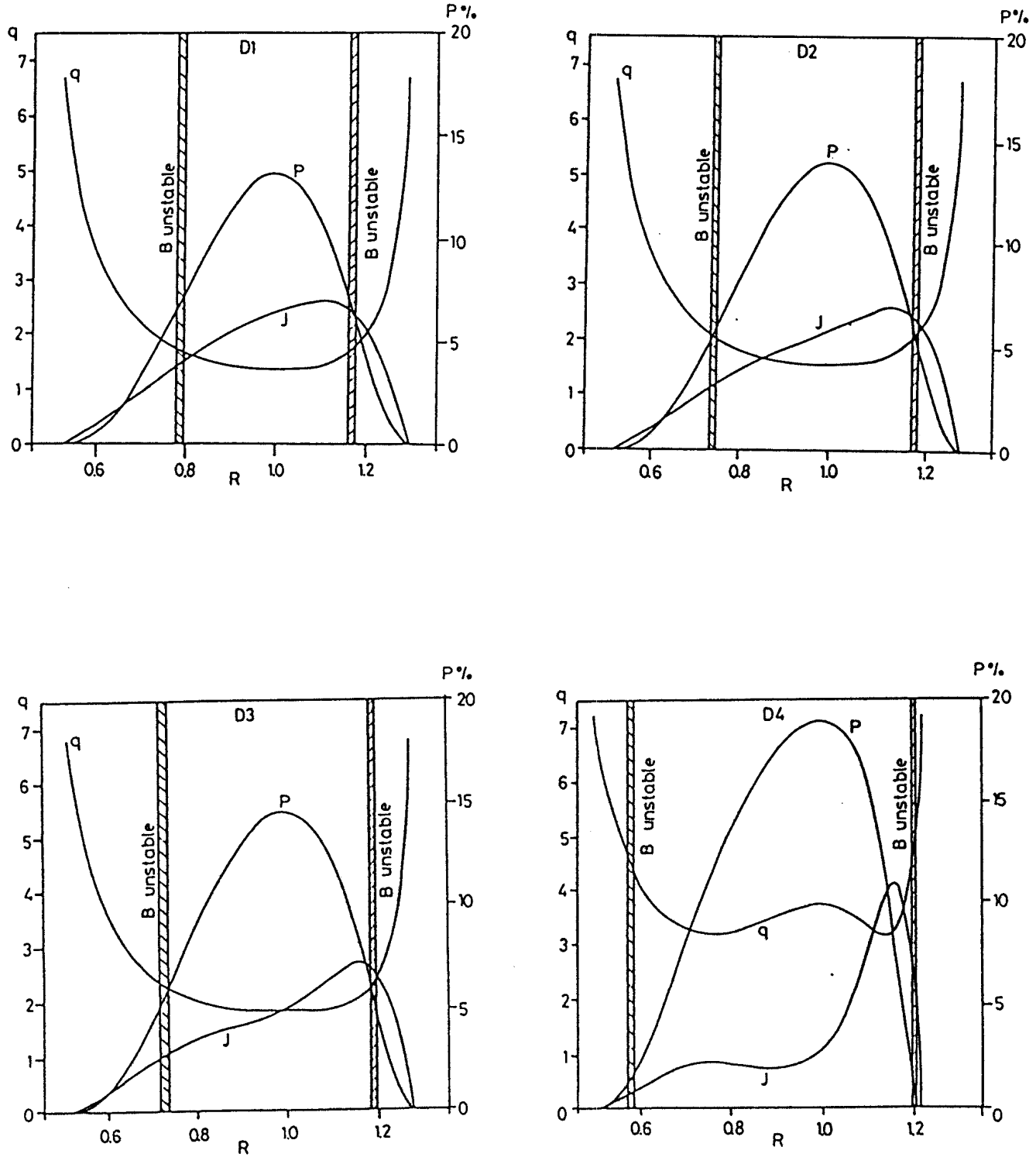
D1
D2
D3
D4
q
P
J
P%
R
B unstable
B unstable
0.6
0.8
1.0
1.2
0
1
2
3
4
5
6
7
0
5
10
15
20

FIG. 4

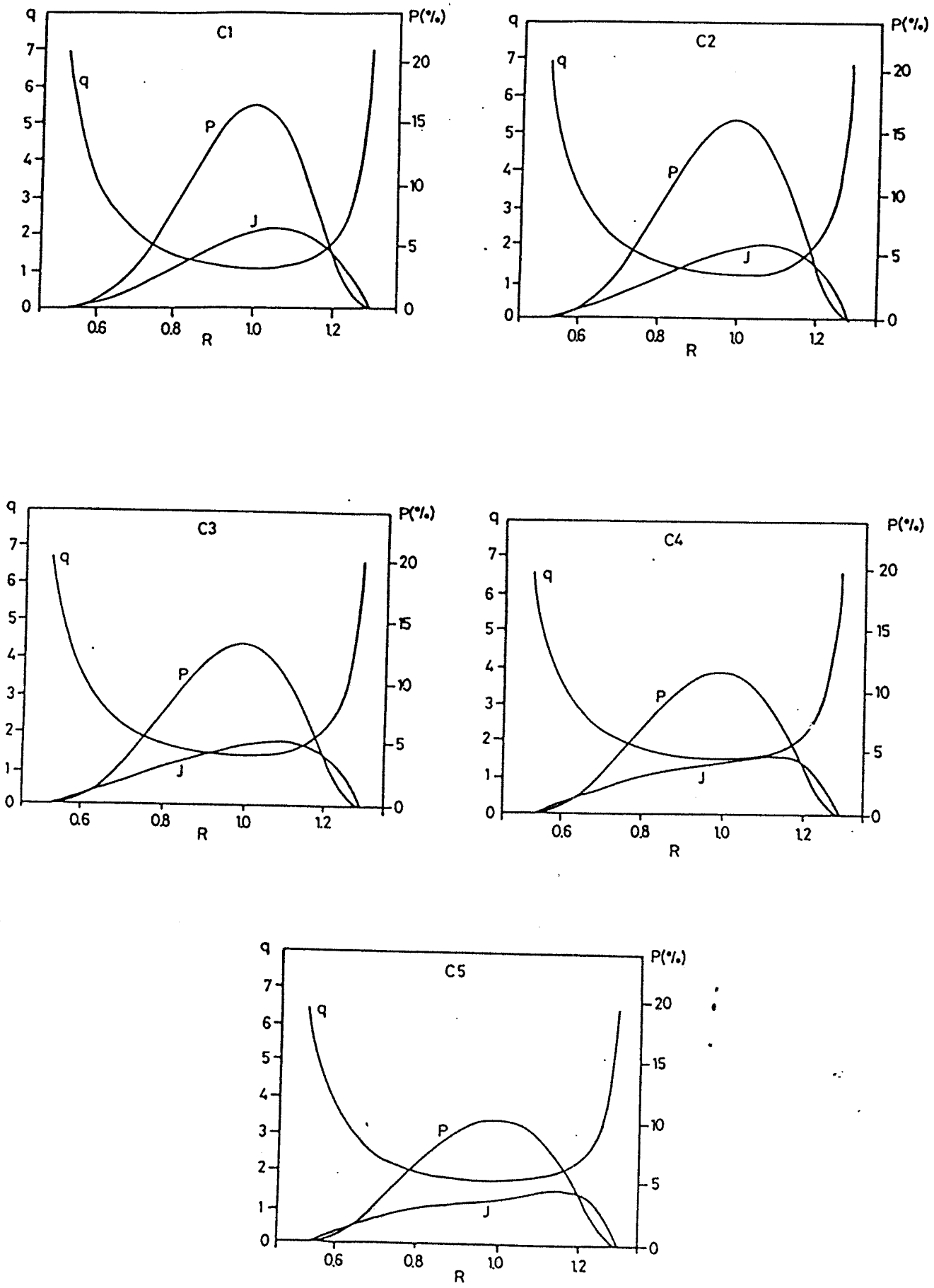

FIG. 5

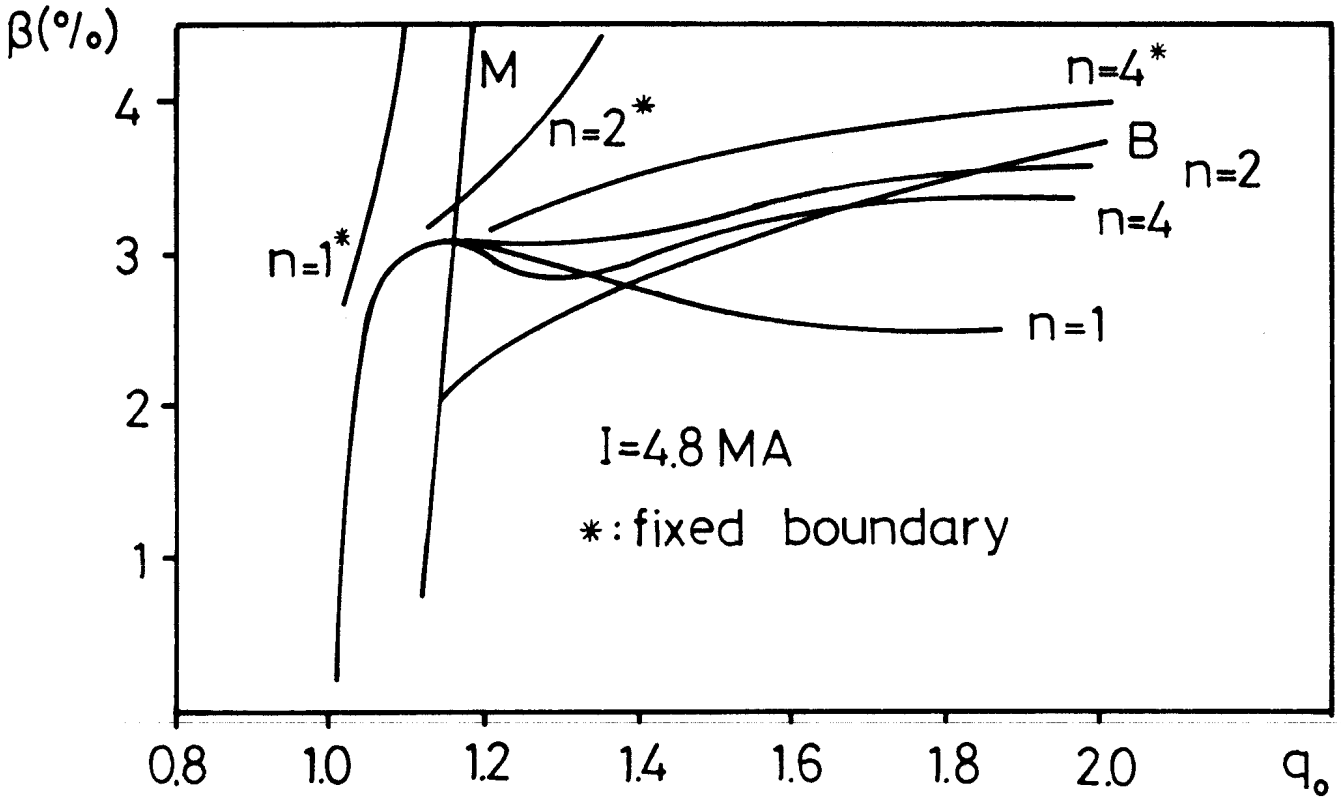
β(%)
4
3
2
1
M
n=2*
n=4*
B
n=2
n=4
n=1*
n=1
I=4.8 MA
*: fixed boundary
0.8
1.0
1.2
1.4
1.6
1.8
2.0
q₀

FIG. 6

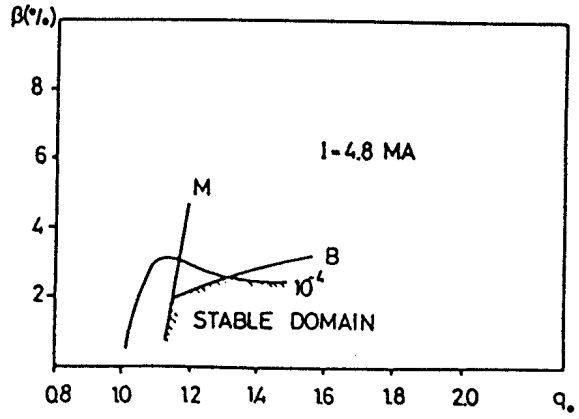
β(%)
8
6
4
2
I = 4.8 MA
M
B
10^{-4}
STABLE DOMAIN
0.8
1.0
1.2
1.4
1.6
1.8
2.0
q_*

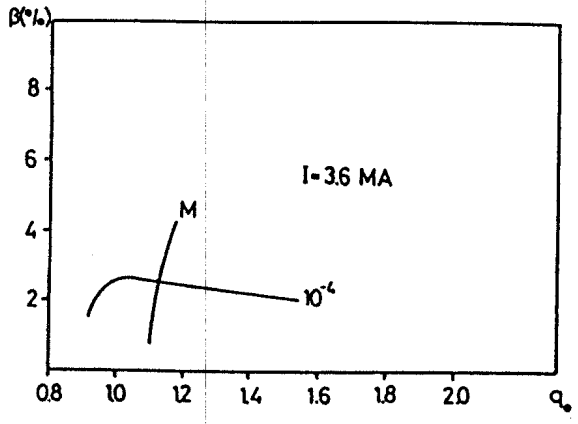
β(%)
8
6
4
2
I = 3.6 MA
M
10^{-4}
0.8
1.0
1.2
1.4
1.6
1.8
2.0
q_*

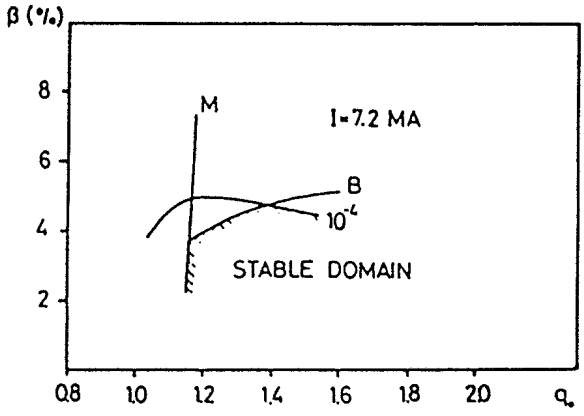
β (%)
8
6
4
2
I = 7.2 MA
M
B
10^{-4}
STABLE DOMAIN
0.8
1.0
1.2
1.4
1.6
1.8
2.0
q_*

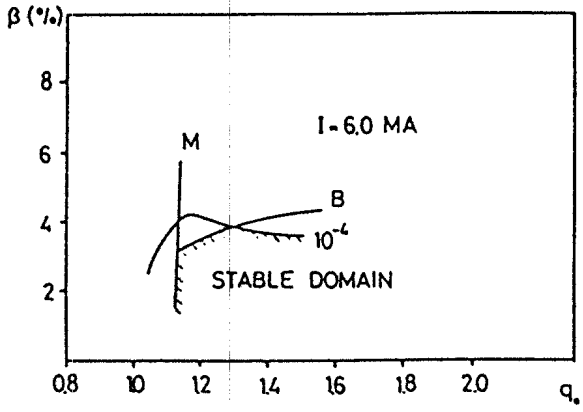
β (%)
8
6
4
2
I = 6.0 MA
M
B
10^{-4}
STABLE DOMAIN
0.8
1.0
1.2
1.4
1.6
1.8
2.0
q_*

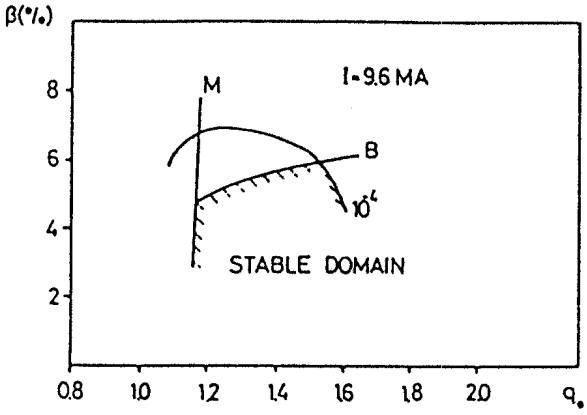
β(%)
8
6
4
2
I = 9.6 MA
M
B
10^{-4}
STABLE DOMAIN
0.8
1.0
1.2
1.4
1.6
1.8
2.0
q_*

FIG. 7

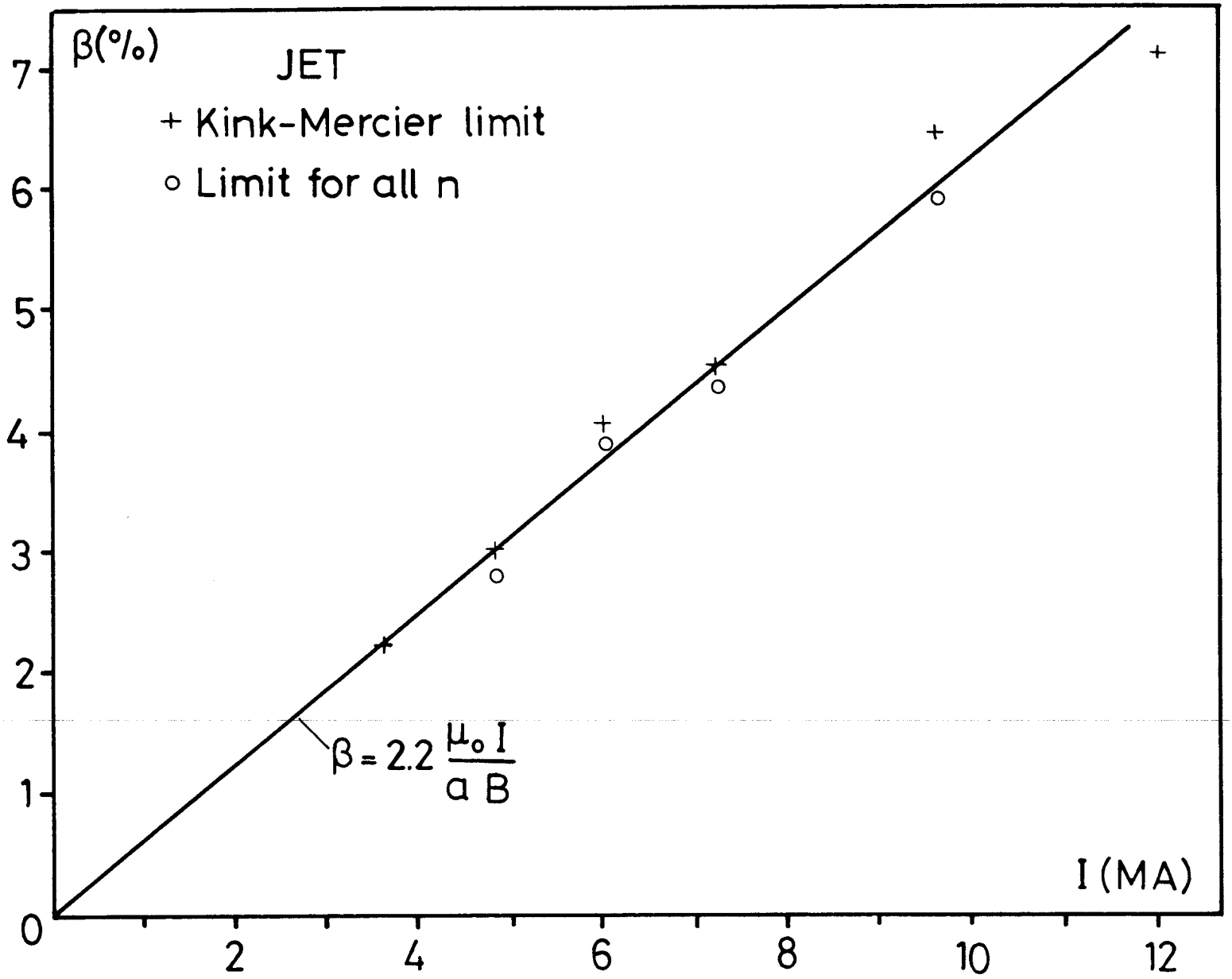
β(%)
JET
+ Kink-Mercier limit
○ Limit for all n
$\beta = 2.2 \frac{\mu_0 I}{a B}$
I (MA)
0
1
2
3
4
5
6
7
2
4
6
8
10
12

FIG. 8

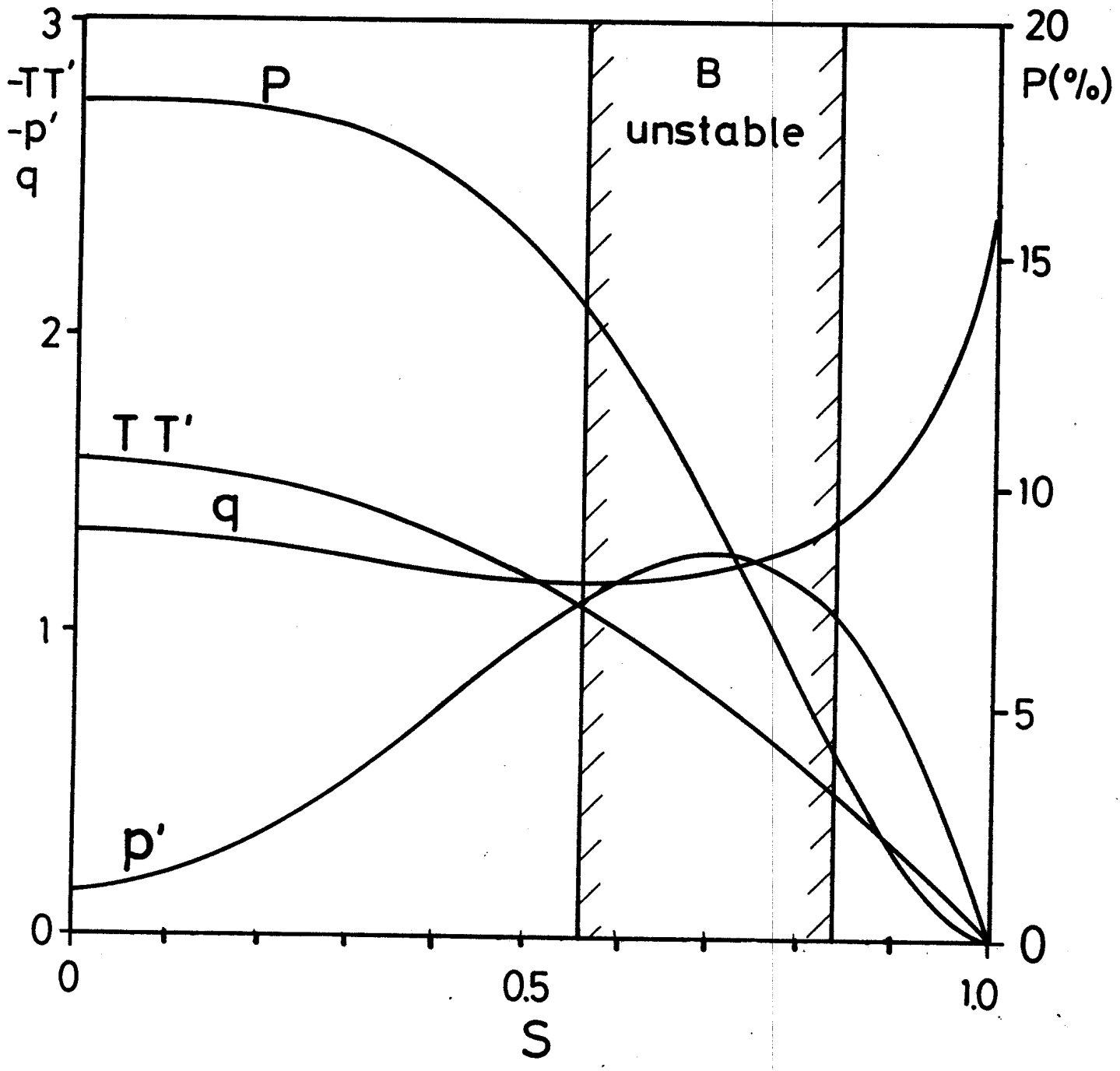

FIG. 9A

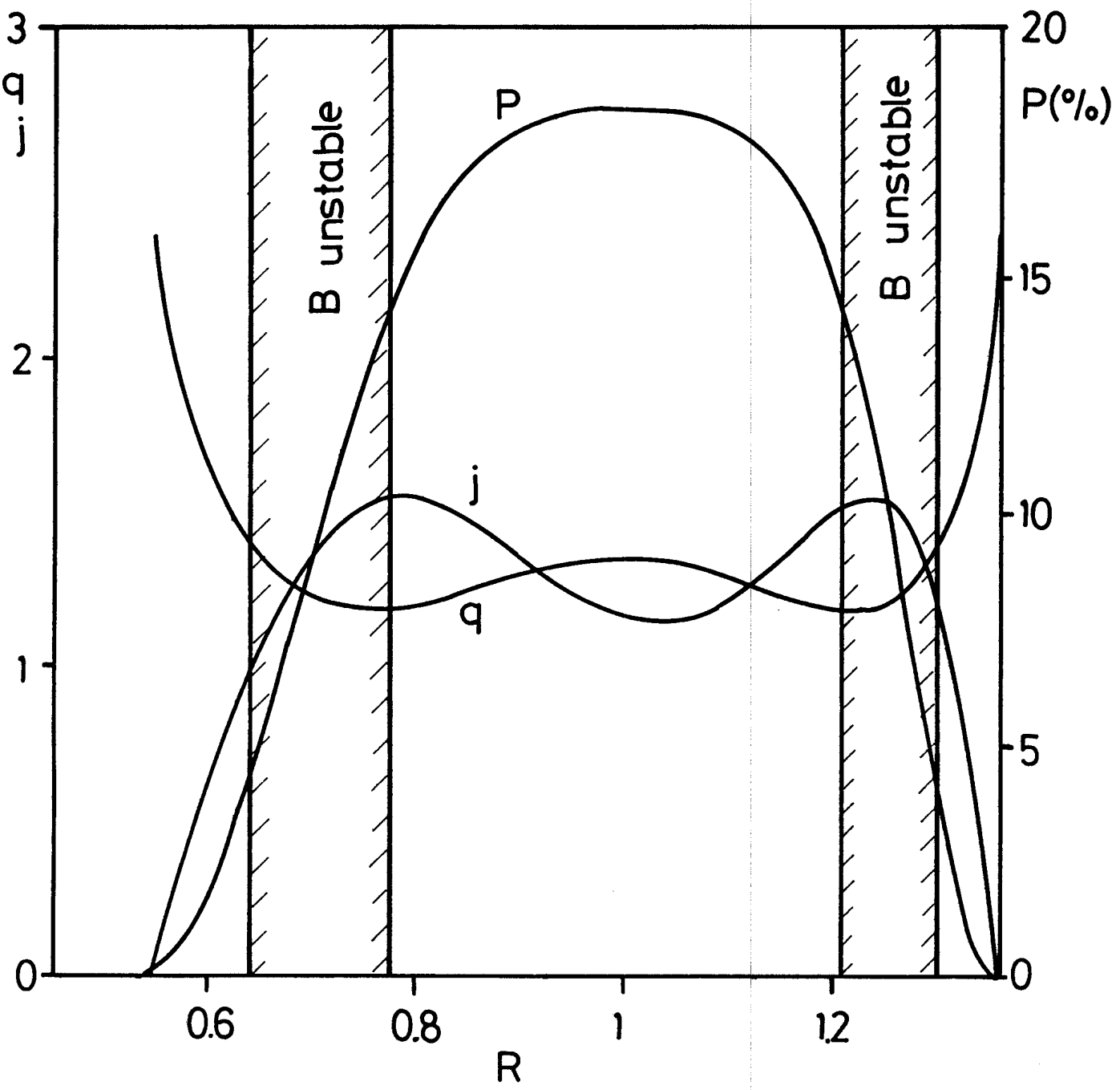

FIG. 9B

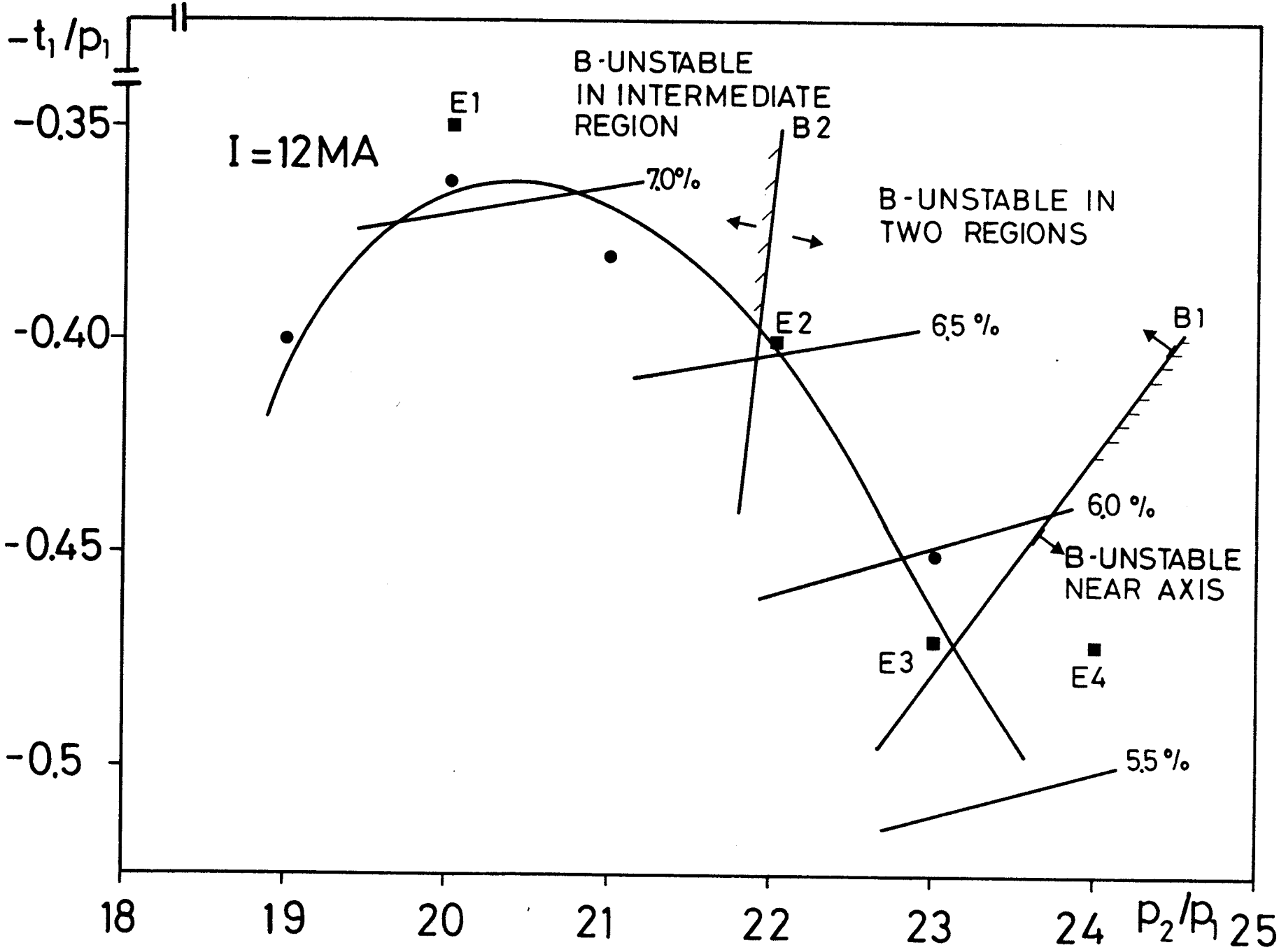
$-t_1/p_1$
-0.35
-0.40
-0.45
-0.5
I = 12MA
E1
B-UNSTABLE
IN INTERMEDIATE
REGION
B2
7.0%
B-UNSTABLE IN
TWO REGIONS
E2
6.5 %
B1
6.0 %
B-UNSTABLE
NEAR AXIS
E3
E4
5.5 %
18
19
20
21
22
23
24
P_2/P_1
25

FIG. 10

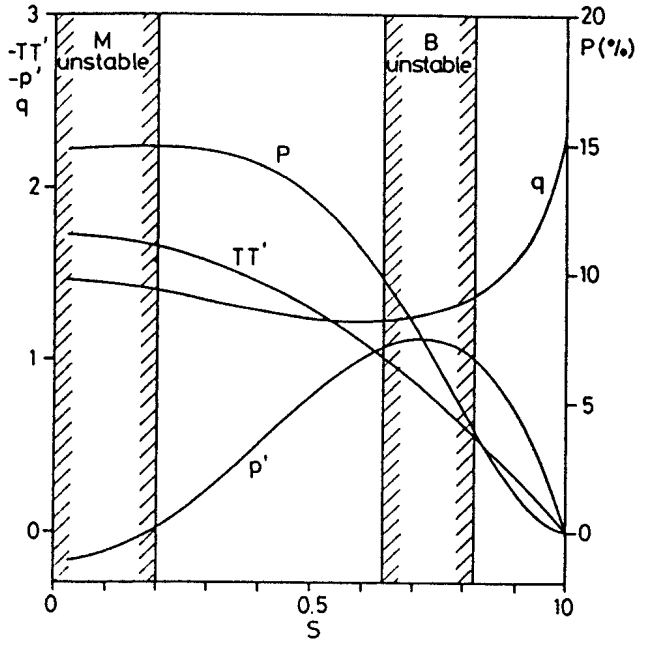
3
-TT'
-p'
q
M
unstable
B
unstable
P(%)
P
TT'
q
p'
0
0.5
1.0
S

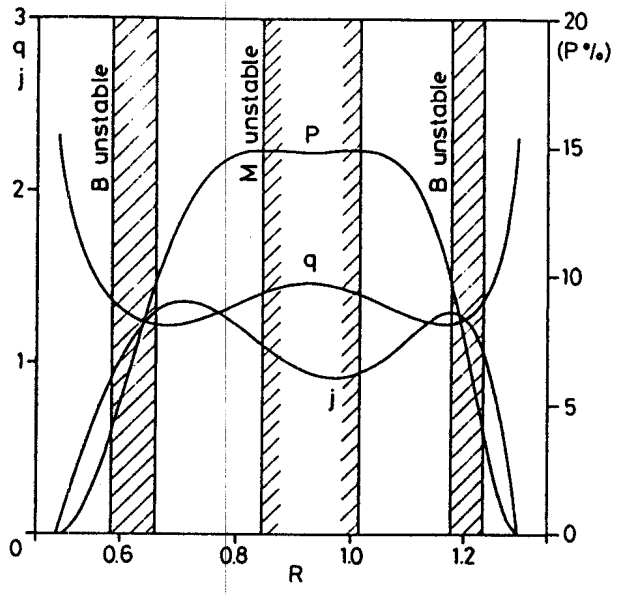
q
j
B unstable
M unstable
B unstable
P
q
j
(P%)
0.6
0.8
1.0
1.2
R

E2

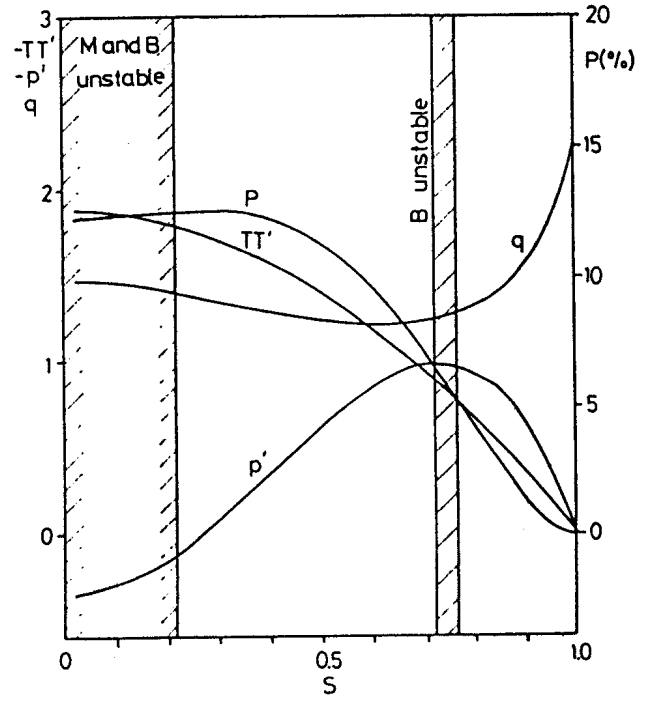
3
-TT'
-p'
q
M and B
unstable
B unstable
P(%)
P
TT'
q
p'
0
0.5
1.0
S

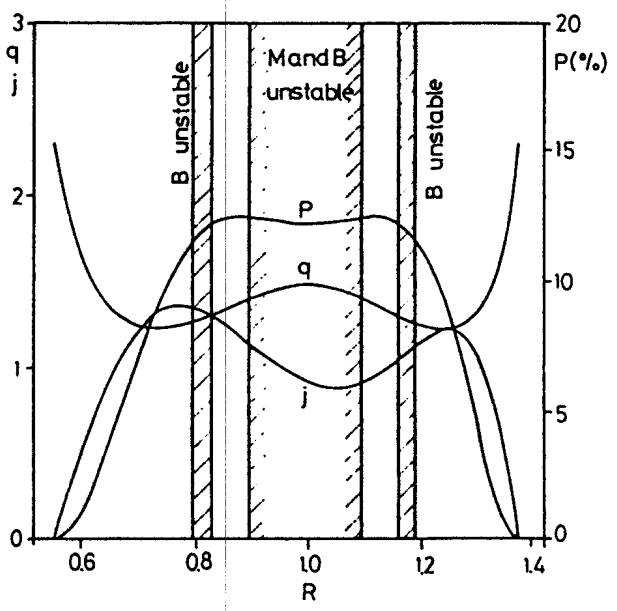
q
j
B unstable
M and B
unstable
B unstable
P(%)
P
q
j
0.6
0.8
1.0
1.2
1.4
R

E3

FIG. 11

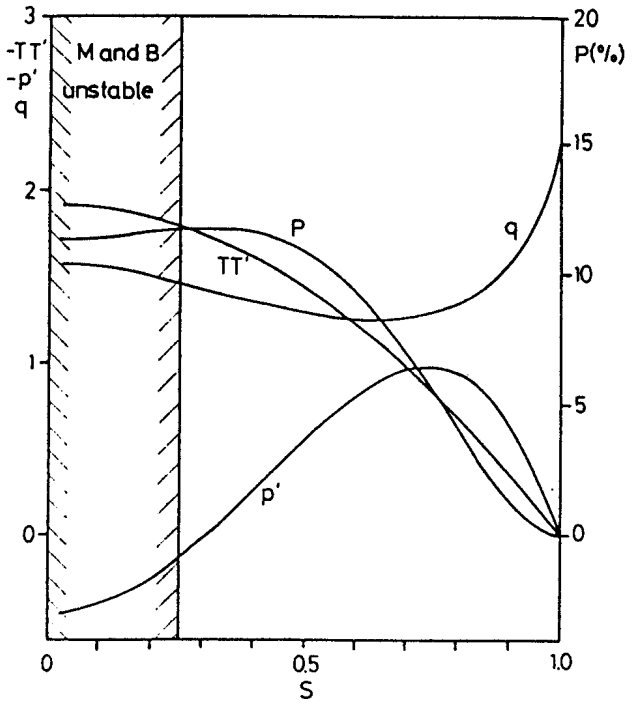

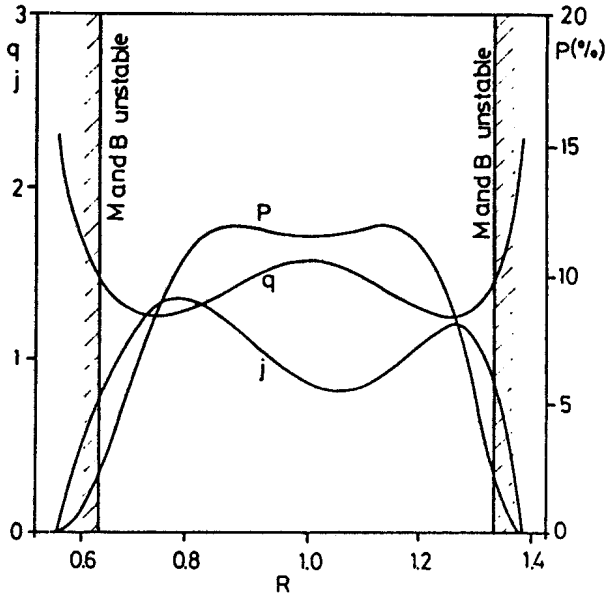

E4

FIG. 11 (CONT'D)